Frequenz
59 (2005)
5-6

Thin-film microstrip lines and coplanar waveguides on semiconductor substrates for sub-mm wave frequencies*

By Frank Schnieder and Wolfgang Heinrich

Dedicated to Professor Hans Brand on the occasion of his 75th birthday
and to Professor Siegfried Martius on the occasion of his 65th birthday

Abstract – It is shown that both thin-film microstrip lines (TFMSLs) and miniaturized coplanar waveguides (CPWs) offer low-dispersive propagation properties up to 1 THz. At the same time, they are fully compatible with monolithic integration. Radiation and dispersion effects are discussed and basic rules are presented how CPWs should be designed in order to reach the desired sub-mm-wave performance.

Index Terms – thin-film microstrip line, coplanar waveguide, MMIC, modeling

1. Introduction

So far, most sub-mm-wave systems have been realized as hybrid circuits. But any interconnect between the components causes parasitics and even those structures which are well suited for microwave frequencies may become critical in the Terahertz range. Therefore, as many elements as possible should be integrated together with the semiconductor devices on the chip. For this purpose, transmission-line structures are required that offer low dispersion together with reasonably low loss. At the same time, they must be compatible with the common planar circuit geometry and processing scheme.

Particular candidates are the coplanar waveguide (CPW) and the thin-film microstrip line (TFMSL), which are realized on top of the chip substrate [1][2][3]. Whereas the common microstrip line uses the whole semiconductor substrate as dielectric layer, in the TFMSL this layer consists of thin dielectric material on top of the semiconductor substrate, e. g. polyimide or BCB (bisbenzocyclobutene), with 1..20 µm thickness. This allows to scale down strip width and thus the total line dimensions. Our investigations show that such thin-film microstrip lines can be used up to 1 THz with excellently low dispersion. Coplanar waveguides with scaled-down dimensions achieve similar properties. Additional to the common CPW design criteria, however, one has to take into account higher-order modes and radiation loss.

2. Thin-film microstrip line (TFMSL)

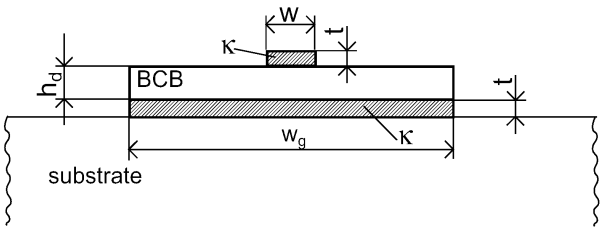

Fig. 1: TFMSL cross-section. κ denotes metal conductivity, the conductor thickness is t = 0.8 µm, ground width $w_g >> w$. 5 Ωcm silicon is used as a substrate and BCB as dielectric.

The TFMSL is the miniaturized version of the conventional microstrip line. Fig. 1 shows its cross section. The fields are concentrated in the dielectric layer and the ground metalization provides shielding against the substrate. Therefore, one may use lossy material as a substrate, e.g., low-resistivity silicon. The typical BCB or polyimide thicknesses are in the range 1…25 µm. This is considerably smaller than for the conventional microstrip case. As a consequence, the line dimensions, i.e., strip width, can be scaled down, which increases the frequency range of quasi-TEM operation well into the Terahertz region. One has to pay for this, of course, by larger attenuation due to conductor loss.

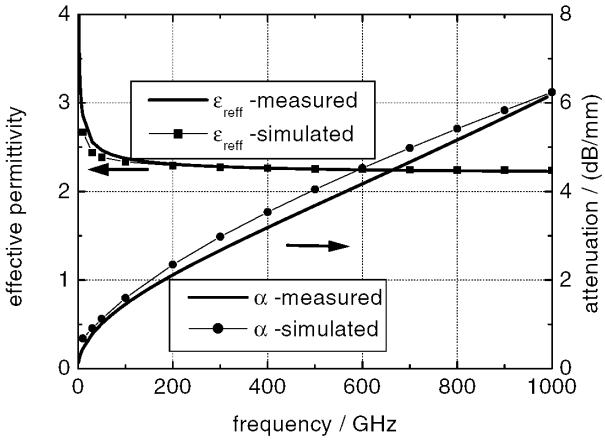

Fig. 2: Effective relative permittivity ε_{reff} and attenuation α as a function of frequency (50 Ω TFMSL according to Fig. 1 with strip width w = 7.4 µm, BCB layer with thickness h_d = 2.7 µm, $\tan\delta_\varepsilon$ = 0.015, and metal conductivity κ = 30 S/µm; Si substrate with ρ = 5 Ωcm; simulation data [5] and electro-optic measurements [4]).

Fig. 2 presents the propagation properties for such a TFMSL with 2.7 µm thick BCB dielectric. The 7.4 µm wide strip yields 50 Ω characteristic impedance. The experimental data refers to electro-optic measurements at the RWTH Aachen [4]. For simulation, our equivalent-circuit model of the TFMSL [5] is applied. This model was created on the basis of electromagnetic full-wave simulations and describes these lines with closed-form expressions up to sub-millimeter-wave frequencies. It is an extension of conventional microstrip models. Electric and magnetic fields inside the metallic conductors are taken into account, because their penetration depth corresponds to the geometric dimensions of the conductors. Besides, the thickness ratio between signal conductor and dielectric layer for TFMSLs is much larger than for conventional microstrip lines.

Effective permittivity $\varepsilon_{reff} = (\beta/\beta_0)^2$ and attenuation α are plotted against frequency up to 1 THz. Effective permittivity exhibits a negative slope at the lower frequency end, which is caused by metal loss, and then approaches a constant value. This demonstrates the quasi-TEM properties and the excellently low dispersion. The reasons are the small BCB thickness and strip width together with the low permittivity of the BCB (ε_r = 2.7). On the other hand, the miniaturized conductor dimensions lead to attenuation values of about 5 dB/mm at 1 THz. However, for short

* This work was supported by the Deutsche Forschungsgemeinschaft under Contract He 1676/10.

connecting lines within an integrated circuit, this is acceptable. Moreover, one can trade lower loss for higher dispersion by increasing the line dimensions.

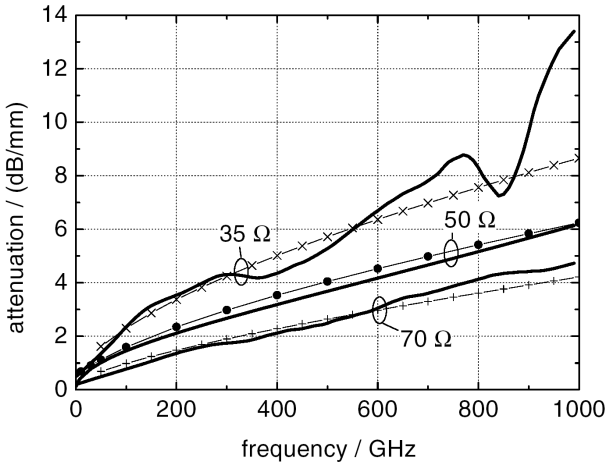

Fig. 3: Attenuation as a function of frequency for a 35 Ω, 50 Ω, and a 70 Ω TFMSL (all data as in Fig. 2, except for w = 8 µm, h_d = 1.7 µm for the 35 Ω case, and w = 8 µm, h_d = 5.4 µm for the 70 Ω line; solid line: measurements, lines + symbols: simulation).

The characteristic impedance can be adjusted by choosing a suitable w/h_d ratio. Fig. 3 illustrates the attenuation curves for the 50 Ω TFMSL of Fig. 2 together with a 35 Ω and a 70 Ω geometry. Larger impedance values can be achieved by increasing h_d or decreasing w. One should note that, despite of the low-ε_r dielectric, the full impedance range down to 30 Ω can be realized within the common technological limitations.

3. Coplanar waveguide (CPW)

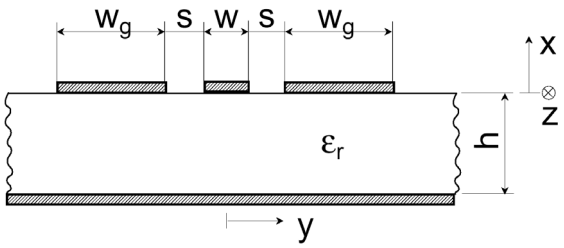

Fig. 4: The CPW geometry considered (substrate: high-resistivity Si with ε_r = 11.67).

The CPW type most appropriate for sub-mm-wave applications is that with finite ground width and substrate thickness. Fig. 4 illustrates the cross-section. As for the TFMSL, high-resistivity silicon is used as a substrate. The substrate resistivity plays an important role in the CPW case, because, in contrast to the TFMSL, the fields penetrate deeply into the substrate and thus attenuation is strongly affected by substrate material loss.

In order to keep dispersion and non-TEM effects low the ground-to-ground spacing $w + 2s$ has to be scaled down with increasing frequency of operation as well as the total line width $w + 2s + 2w_g$.

Figs. 5 and 6 present simulation results and electro-optic measurements [4] for such a miniaturized CPW in the frequency range up to 1 THz. Two different ground-plane widths w_g of 160 µm and 16 µm are studied. Generally, dispersion in ε_{reff} is small but larger than for the TFMSL structures treated before. This can be attributed to the larger lateral line dimensions of the CPW (note that the CPW ground-to-ground spacing $w + 2s$ in Figs. 5 and 6 is 40 µm compared to 8 µm strip width for the TFMSL in Figs. 2 and 3). In the lower GHz range, one has the typical increase in ε_{reff} caused by conductor loss as observed for the TFMSL. More important, however, are the attenuation results. They show clearly that the reduced ground width leads to a considerably lower attenuation level at high frequencies.

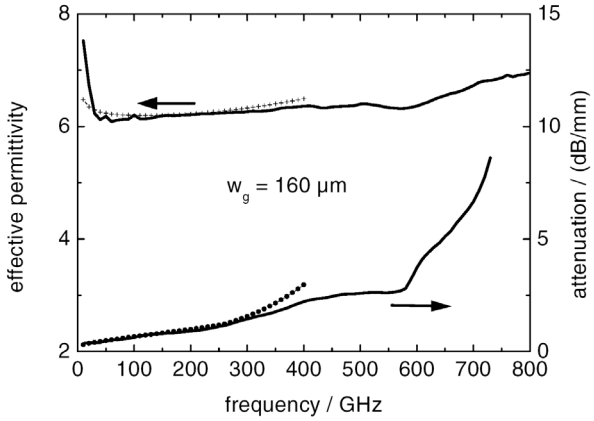

Fig. 5: Effective relative permittivity and attenuation as a function of frequency for a CPW with wide ground-planes. (solid lines: electro-optic measurements [4], symbols: analytic model simulation [7]). For geometry and parameters see Fig. 4 with w = 16 µm, s = 12 µm, w_g = 160 µm, metal conductivity 35 S/µm, 380 µm thick Si substrate).

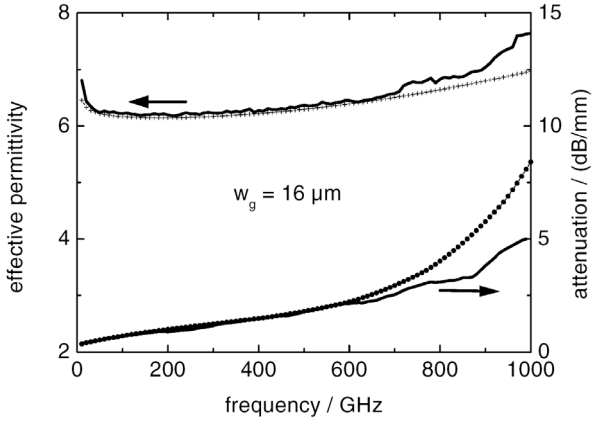

Fig. 6: Effective relative permittivity and attenuation as a function of frequency for a CPW with narrow ground-planes. (solid lines: electro-optic measurements [4], symbols: analytic model simulation [7]). For geometry and parameters see Fig. 4 and caption of Fig. 5 except for w_g = 16 µm.

The simulation data were calculated by our quasi-static CPW model [6][7]. It is a comprehensive and efficient CPW description accounting for all relevant effects from conductor, substrate, and radiation loss to high-frequency dispersion. Similar to the TFMSL model, also the fields in the conductors are considered. Additionally, the emission of electromagnetic energy into the substrate of the line becomes important at sub-mm-wave frequencies and has to be included in the CPW model. The model in closed form, as described before, can be used up to the frequencies, when higher-order modes interact with the CPW mode. This will be explained later in the context of Fig. 7. For the CPW with w_g = 160 µm this frequency limit is at about 360 GHz, whereas for the CPW with w_g = 16 µm the analytic model delivers results which fit the measurements up to double the frequency.

In the CPW case, one has not only to account for dispersion and radiation of the CPW mode but also to consider higher-order modes, which may adversely affect propagation characteristics or cause parasitic effects in the packaged circuit (see, e.g., [8]). These higher-order modes are related to substrate thickness h and ground width w_g [9].

For ground planes of infinite extent ($w_g = \infty$) radiation into lateral surface-wave modes starts already at the frequency f = 0. Finite ground conductor width ($w_g < \infty$) causes a shift of the onset of radiation to higher frequencies, but it does not prevent the existence of a parallel-plate like (PPL) mode (sometimes referred

to as the microstrip-like mode). This PPL mode is present in any case as long as conductor-backed substrates are used. In practical circuits, the PPL mode forms a parasitic bypass between discontinuities and interconnects, which reduces isolation and may cause instabilities in high-gain systems.

The third fundamental mode of the CPW structure in Fig. 4 is the slot-line mode. In reality it can be suppressed by airbridges, which connect the two ground conductors on top of the line structure electrically. In the numerical investigations a magnetic symmetry wall is assumed in the center of the line structure and only one half of the whole structure is analyzed.

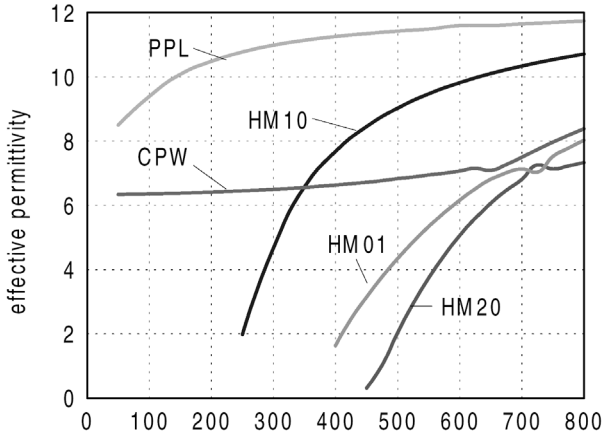

Fig. 7: Effective relative permittivity of fundamental modes (CPW, PPL) and higher-order modes (HM) against frequency (FDFD analysis of the geometry in Fig. 4 with ideally conducting metalizations, w = 16 µm, s = 12 µm, w_g = 80 µm, and h = 200 µm).

Fig. 7 presents the effective relative permittivity values for the remaining two fundamental modes (CPW and PPL) and the first three higher-order ones (HM). A CPW structure similar to the structures in Figs. 5 and 6 is analyzed by means of full-wave electromagnetic simulation using FDFD (finite difference frequency domain) method [10][11].

One finds that the PPL mode exhibits a microstrip-like dispersion behavior with a strong increase in ε_{reff} with growing frequency, whereas the CPW effective permittivity remains almost constant up to about 600 GHz in this case. Here, the critical effect is not non-TEM dispersion itself, but interaction with higher-order modes.

For the geometry studied in Fig. 7, the first higher-order modes HM10 as well as HM20 are related to substrate thickness h, i.e., they can be shifted towards higher frequencies by reducing h. The second type of higher-order mode, HM01, is due to the lateral line width, i.e., primarily ground-plane width w_g. Thus, one concludes that for reliable high-frequency operation, both h and w_g have to be chosen small enough to prevent the occurrence of higher-order modes. Introducing an approximate model one derives a simple formula providing the corresponding design values as a function of the desired maximum frequency of operation f_{max} [9]:

$$\max\left\{h, \frac{w}{2}+s+w_g\right\} \le \frac{1}{f_{max}\cdot\sqrt{2\mu_0\varepsilon_0(\varepsilon_r-1)}} \qquad (1)$$

Using (1) one can easily adjust substrate thickness h and ground-width w_g to the desired frequency range. Note that a further reduction of w_g can be of advantage, because it reduces attenuation (see Figs. 5 and 6). Furthermore, one should note that not each higher-order mode interacts with the CPW mode. A condition for the interaction between modes is not only a comparable value of effective relative permittivity, but also a similar attenuation value. This second condition is not fulfilled for the HM10 mode in Fig. 7, for instance. That is why (1) represents a limit for a secure operation of the CPW, but does not mean that one necessarily has strong mode interaction when exceeding these limits.

4. CPW versus TFMSL

As described in the preceding sections, CPW and TFMSL both are suitable sub-mm-wave transmission lines. A direct comparison is presented in Fig. 8, considering the propagation properties of the two different lines, calculated by means of our analytic models [5][7]. In order to obtain useful information from such a comparison, two structures are compared that provide the same characte-ristic impedance and are comparable in size. The latter condition involves some uncertainties as to lateral line size. In the CPW case (see Fig. 4), the total line width ($w + 2s + 2w_g$) represents a good measure, also regarding the lateral spacing from neighboring lines required to prevent crosstalk.

For the TFMSL, it is more difficult to define such a figure since the strip width w (see Fig. 1) is much smaller than the spacing needed because of crosstalk. A value of 5 times the dielectric thickness h_d gives good isolation so that the total width allocated by a TFMSL is approximately $10h_d + w$. Following these considerations, in Fig. 8 both for CPW line width ($w + 2s + 2w_g$) and TFMSL width ($10h_d + w$) the same value of 62 µm is chosen [12].

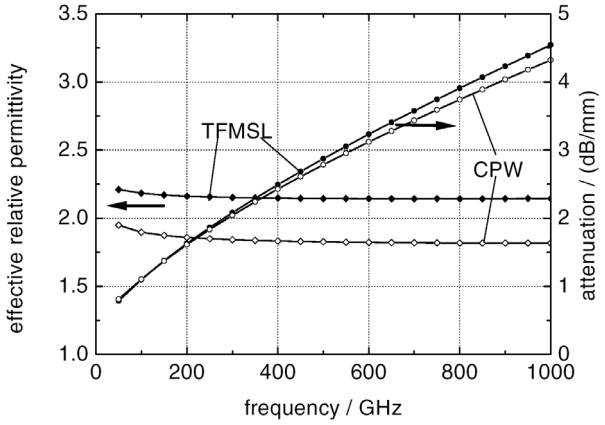

Fig. 8: Comparison of CPW and TFMSL (70 Ω lines of equivalent size): effective relative permittivity and attenuation against frequency (simulation data [5][7]); TFMSL dimensions as in Fig. 1 with w = 8 µm, h_d = 5.4 µm, CPW as in Fig. 4 with w = 13 µm, s = 3.5 µm, w_g = 21 µm on 25 µm thick BCB over 5 Ωcm Si substrate, Al metalization with κ = 23.5 S/µm, BCB: ε_r = 2.7, $\tan\delta_\varepsilon$ = 0.015.

The results demonstrate that both line types show comparable attenuation. The same statement holds for dispersion characteristics, which is negligible up to at least 800 GHz. Naturally, effective permittivity for the CPW is lower than for the TFMSL, because in the latter case the field portion within the dielectric is larger. Briefly speaking, the differences with respect to dispersion and attenuation are minor and do not justify a clear preference for one of the line types.

There is one major difference, however, which is important for circuit design: The BCB dielectric with its low permittivity value is very beneficial in reducing dispersion. But, at the same time, it lowers characteristic impedance for a given conductor geometry. So, given a fixed impedance value, e.g., 50 Ω, one has to compensate for this by adjusting conductor dimensions accordingly. For the TFMSL, this is obtained easily (see Figs. 2 and 3). For the CPW, however, this requires a very small slot-to-strip width ratio s/w.

This can be seen from the data in Fig. 8, where for a 70 Ω CPW a slot width of only 3.5 µm is necessary. For a 50 Ω CPW, situation is worse: assuming 40 µm ground-to-ground spacing (as treated in Section 3) on a dielectric with ε_r = 2.7 yields a center

strip width w of 35 µm and a slot width s = 2.5 µm, which is at the technological limits of the common processes. Thus, on low-ε_r dielectrics, the realistic impedance range of the CPW is shifted towards values beyond 50 Ω.

5. Conclusions

- Both TFMSL and miniaturized CPW are suitable for sub-mm-wave monolithic applications. Scaling down the dimensions yields excellent dispersion properties and low radiation, of course, at the expense of higher conductor loss. Attenuation levels are in the range of 5..10 dB/mm at 1 THz. Given the short line lengths in monolithic structures this is acceptable.
- While TFMSL and CPW achieve comparable performance in terms of dispersion and loss, there are differences in flexibility. The TFMSL properties do not depend on substrate quality and it covers a wider impedance range. The CPW impedance range, on the other hand, is restricted more severely by technological limitations, particularly the minimum slot width. This causes problems when realizing CPWs on low-permittivity dielectrics. Then the 50 Ω value may be below the available impedance range.

References

[1] F. J. Schmückle, A. Jentzsch, H. Oppermann, K. Riepe, W. Heinrich: W-band flip-chip interconnects on thin-film substrate. 2002 IEEE MTT-S Int. Microwave Symp. Digest, pp. 1393-1396.

[2] M. Steinhauer, H. Irion, M. Schott, M. Thiel, H.-O. Ruoss, W. Heinrich: SiGe-based circuits for sensor applications beyond 100 GHz. 2004 IEEE MTT-S Int. Microwave Symp. Digest, vol. 1, pp. 223-226.

[3] S.-N. Lee, O.-G. Lim, J.-G. Yook, Y.-J. Kim: High performance elevated thin-film microstrip on polyimide-loaded silicon. 33rd European Microwave Conf. Munich, 2003, pp. 659-662.

[4] H.-M. Heiliger, M. Nagel, M. Setz, H. G. Roskos, H. Kurz, F. Schnieder, W. Heinrich: Thin-film microstrip lines for mm and sub-mm-wave on-chip interconnects. 1997 IEEE MTT-S Int. Microwave Symp. Digest, vol. 2, pp. 421-424.

[5] F. Schnieder, W. Heinrich: Model of thin-film microstrip line for circuit design. IEEE Trans. Microwave Theory Techn., 49 (2001) 1, pp. 104-110.

[6] W. Heinrich: Quasi-TEM description of MMIC coplanar lines including conductor loss effects. IEEE Trans. Microwave Theory Techn., 41 (1993) 1, pp. 45-52.

[7] F. Schnieder, T. Tischler, W. Heinrich: Modeling dispersion and radiation characteristics of conductor-backed CPW with finite ground width. IEEE Trans. Microwave Theory Techn., 51 (2003) 1, pp. 137-143.

[8] H. Shigesawa, M. Tsuji, A. A. Oliner: Conductor-backed slot line and coplanar waveguide: dangers and full-wave analyses, 1988 IEEE MTT-S Int. Microwave Symp. Digest, vol. 1, pp. 199-202.

[9] W. Heinrich, F. Schnieder, T. Tischler: Dispersion and radiation characteristics of conductor-backed CPW with finite ground width. 2000 IEEE MTT-S International Microwave Symposium Digest, Boston, vol. 3, pp. 1663-1666.

[10] T. Tischler: Die Perfectly-Matched-Layer Randbedingung in der Finite-Differenzen-Methode im Frequenzbereich: Implementierung und Einsatzbereiche. Innovationen mit Mikrowellen & Licht, Forschungsberichte aus dem Ferdinand-Braun-Institut für Höchstfrequenztechnik Berlin, Band 1. Cuvillier Verlag, Göttingen 2004, also http://edocs.tu-berlin.de/diss/2003/tischler_thorsten.htm.

[11] T. Tischler, W. Heinrich: The perfectly matched layer as lateral boundary in finite-difference transmission-line analysis. IEEE Trans. Microwave Theory Tech. 48 (2000) 12, pp 2249–2253.

[12] F. Schnieder, W. Heinrich: Low-dispersive coplanar waveguide and thin-film microstrip lines for sub-mm wave monolithic integration. 8th International Conf. on Terahertz Electronics, Darmstadt, 28-29 Sept. 2000, VDE Verlag Berlin 2000, pp. 165-168.

Acknowledgements

Part of this work was pursued in a collaboration with the RWTH Aachen, Lehrstuhl für Halbleitertechnik II (Prof. H. Kurz), where the TFMSL and CPW structures were fabricated and the electro-optic measurements were performed. The authors gratefully acknowledge this and would like to thank particularly H. Roskos, H.-M. Heiliger, and T. Pfeiffer for their contributions.

Frank Schnieder
Wolfgang Heinrich
Ferdinand-Braun-Institut für Höchstfrequenztechnik (FBH)
Gustav-Kirchhoff-Str. 4
12489 Berlin
Germany
Fax: +49 (30) 63 92-26 42
E-Mail: wolfgang.heinrich@fbh-berlin.de

(Received on April 8, 2005)